Proc. Natl. Acad. Sci. USA
Vol. 78, No. 11, pp. 6996–6999, November 1981
Developmental Biology

Morphometric aspects of ciliary distribution and ciliogenesis in human nasal epithelium

(respiratory epithelium/cilia/freeze-fracture/morphometry)

JOHNNY L. CARSON*†, ALBERT M. COLLIER*†‡, MICHAEL R. KNOWLES§, RICHARD C. BOUCHER§, AND JAMES G. ROSE*

*Department of Pediatrics, ‡Frank Porter Graham Child Development Center, †Center for Environmental Health and Medical Sciences, and §Department of Medicine, University of North Carolina, Chapel Hill, North Carolina 27514

Communicated by John N. Couch, July 24, 1981

ABSTRACT **Observations of freeze-fracture preparations of human nasal epithelium have provided a unique perspective of the spatial distribution of epithelial cell cilia unattainable by more conventional ultrastructural techniques. The initial stages of ciliogenesis were characterized ultrastructurally in these preparations by differentiation of the lumenal aspect of the epithelial cell membrane prior to the emergence and maturation of new cilia. Morphometric analyses of the resultant electron micrographs indicate that the development of an optimal ciliary population during differentiation of ciliated cells may be integral to the adequate functioning of respiratory mucociliary mechanisms. The frequency with which such ciliogenic structures are observed indicates that ciliogenesis is a common feature of the nasal epithelium and suggests that epithelial cell turnover in the nasal cavities is relatively rapid.**

Classical models of ciliogenesis in the conducting airway epithelial layer have employed experimental animal models to study this aspect of epithelial cell differentiation. These studies, based on ultrastructural observations of various stages of the developing respiratory system *in vivo* and *in vitro*, indicated that beds of cilia emerge from the epithelial cells during a specific stage of embryological development (1–3). It is generally thought that the portion of cells comprising the mature lumenal border of this pseudostratified columnar epithelium arises through division and differentiation of underlying basal cells into the specialized cell types populating the lumenal border (4). These observations provide a plausible explanation for the embryological generation of ciliary beds lining the conducting airways but do little to account for subsequent differentiation of ciliated cells and ciliogenesis during normal growth and development or in response to injury.

Recent ultrastructural investigations carried out in this laboratory have demonstrated the occurrence of ciliogenesis in the nasal epithelium of normal human subjects. It is clear from these studies that the lumenal membranes of ciliated cells are specifically differentiated prior to the emergence and maturation of cilia. A developmental sequence in the formation of the ciliary necklace (5), a ciliary membrane particle complex, is evident. Initial stages of ciliogenesis are indicated by the formation of prenecklace patches (PNPs) in the lumenal membrane, followed by organization of the particles comprising each patch into the mature ciliary necklace during emergence of the ciliary shaft. Additionally, morphometric studies of the nasal epithelium suggest that a critical distribution of cilia occurs on the lumenal border of ciliated cells which may be integral to the maintenance of mucociliary function.

The publication costs of this article were defrayed in part by page charge payment. This article must therefore be hereby marked "*advertisement*" in accordance with 18 U. S. C. §1734 solely to indicate this fact.

MATERIALS AND METHODS

Informed consent was obtained from the human volunteers participating in these studies. Samples of nasal epithelium from the medial surface of the inferior turbinate were obtained from normal young men and women by the technique described by Alford *et al.* (6). After retrieval, the samples were prepared for freeze-fracture by immediate fixation in 2% (vol/vol) glutaraldehyde/2% (wt/vol) paraformaldehyde in 0.1 M phosphate buffer (pH 7.2), followed by a rinse in 0.1 M phosphate buffer containing 0.2 M sucrose. Prior to freezing, the samples were treated for 1 hr in a cryoprotectant consisting of 25% (vol/vol) glycerol in 0.1 M phosphate buffer. Each sample was then positioned on double-replica specimen stubs, frozen in liquified Freon 22, and stored in liquid nitrogen. Freeze-fracture was performed in a Balzers 360 M device at a stage temperature of −100°C. Replicas were produced by platinum/carbon shadowing at 45° and carbon coating at 90°. Replicas were cleaned in 5% (wt/vol) sodium dichromate in 50% (vol/vol) H_2SO_4 and retrieved from distilled water on copper grids. Samples of inferior turbinate nasal epithelium also were processed for observation of ultrathin sections by postfixation of the aldehyde-fixed tissue in phosphate-buffered 2% (wt/vol) osmium tetroxide, with subsequent dehydration and embedment in Epon 812. Ultrathin sections were cut on an LKB–Huxley ultramicrotome and retrieved on copper grids. All specimens were viewed and photographed on a Zeiss EM-10A transmission electron microscope at an accelerating voltage of 60 kV.

Morphometric determinations were made of ciliary density and center-to-center interaxonemal spacing (see Table 1) in micrographs obtained from freeze-fracture preparations by using a Zeiss Videoplan computer with measuring software. Ciliary density was evaluated by counts of total cross-fractured existing cilia or PNPs, or both, in measured areas of lumenal membrane fractures. Interaxonemal spacing was assessed by determination of the center-to-center distance between an existing cilium or PNP to the nearest neighboring cilium or PNP. Electron micrographs illustrating lumenal border fractures in fields of view varying from portions of one to several adjacent cells and from different individuals were selected at random for evaluation. Ciliary density and mean spacing values were determined in each micrograph, and composite mean values were obtained in each morphometric category (see Table 1). Lumenal borders identified as having either no PNPs or having PNPs numbering less than 10% of the existing cilia were designated by convention as type A profiles (Fig. 1*A*). Profiles from randomly selected areas that showed PNPs numbering 10% or more of the existing cilia were designated by convention as type B profiles (Fig. 1*B*). *Real* or *control* values designated by the

Abbreviation: PNPs, Prenecklace patches.

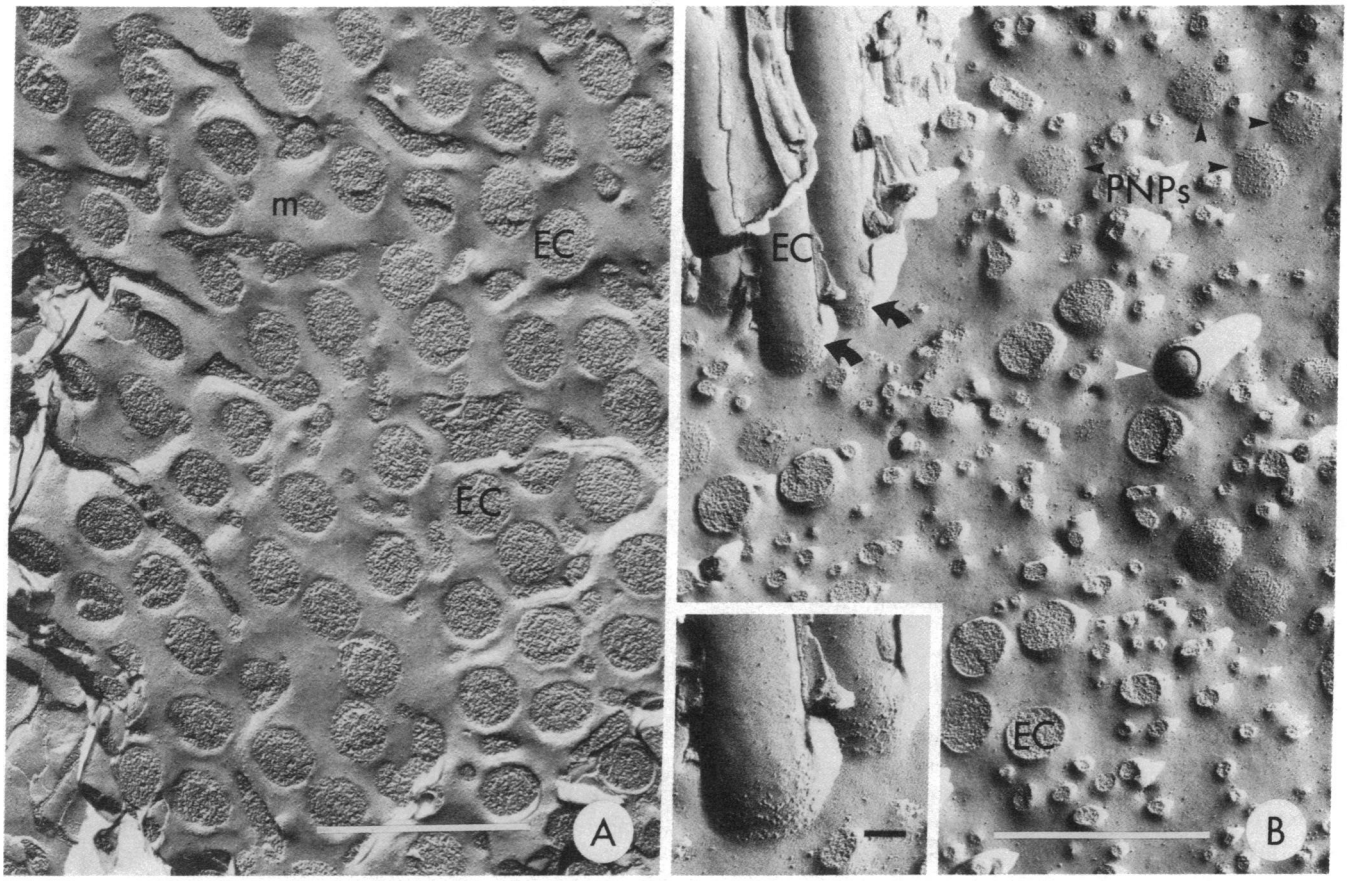

FIG. 1. (*A*) Transmission electron micrograph of a freeze-fracture preparation of normal human nasal epithelium. The fracture plane has passed through the lumenal aspect of the cell membrane shearing existing cilia (EC) and microvilli (m) in cross section. Note the heavy density and close spacing of the cilia and the absence of organized arrays of PNPs indicative of ciliogenesis. This micrograph is representative of a type A profile. Although PNPs may be observed in profiles of this type, they generally appear as a small percentage of the existing cilia. (Bar = 1.0 μm.) (*B*) An electron micrograph obtained from another sample of normal human nasal epithelium. Note that the lumenal surface is only sparsely populated by existing cilia (EC), revealed in both cross and transverse fractures in this micrograph, resulting in low ciliary density and high interaxonemal spacing values. Also evident, however, are a number of circular arrays of membrane-associated particles or PNPs (black arrows) destined to develop into the ciliary necklaces of new cilia. A new, partially emergent cilium with basal necklace particles (white arrow) and mature ciliary necklaces on fully extended cilia (curved arrows) can be seen. This micrograph is representative of a type B profile. The addition of new populations of cilia represented by PNPs to the lumenal border will increase ciliary density and decrease interaxonemal spacing to values approaching those in *A*. (Bar = 1.0 μm.) (*Inset*) Detail of mature ciliary necklaces at higher magnification. (Bar = 0.1 μm.)

morphometric categories represent determinations of density and spacing as seen in cross fractures of existing cilia only. *Predicted* values incorporate the occurrence of PNPs into the density and spacing determinations as representative of cilia that ultimately will populate the lumenal border. For comparison of the various categories, *t*-test statistics were used with a 0.05 level of significance.

RESULTS

Freeze-fracture preparations of normal human nasal epithelium provided a useful technique for visualizing membrane differentiation during ciliogenesis and for enumerating the spatial distributions of both new and previously emerged cilia on the lumenal membrane (Fig. 1 *A* and *B*). P-face fractures of lumenal border membranes demonstrated the aggregation of intramembranous particles into circular patches approximately the diameter of a ciliary shaft (Fig. 2*A*). The arrangement of particles within the patches ranged from a totally random distribution to well-organized concentric arrays suggestive of a developmental sequence of the ciliary necklace prior to the emergence of ciliary shafts (Fig. 2 *B* and *C*). Blebs of the membrane erupting through these particle complexes were indicative of the emergence of new ciliary shafts (Fig. 2*D*). Each particle array defined the ciliary necklace (Fig. 2*E*) (6) of a new cilium as a series of 4–6 rings of particles lying at the base of the cilium.

Ultrathin sections of the nasal mucosa (Fig. 3) showed ciliary buds on the lumenal border above basal bodies. Basal bodies also were distributed throughout the cytoplasm of some lumenal border cells. New basal bodies and ciliary buds were often observed on lumenal border cells having abundant microvillar populations.

Two major types of lumenal border profiles were observed in these studies, from which three categories of morphometric data were derived (Table 1). Some cells had lumenal borders with cross fractures through beds of existing cilia but with little or no apparent expression of ciliogenesis as indicated by the occurrence of PNPs. These fracture surfaces were designated type A profiles and comprised the type A-*control* morphometric category, which provided an estimate of the optimal distribution of cilia on the lumenal border of conducting airway epithelial cells. However, views of other cells revealed cross fractures through existing cilia as well as varying populations of PNPs indicative of active ciliogenesis. These areas were designated as type B profiles (Fig. 1*B*). The type B-*real* morphometric category characterized the distribution of existing cilia on the type B profiles; whereas, the type B-*predicted* category provided an

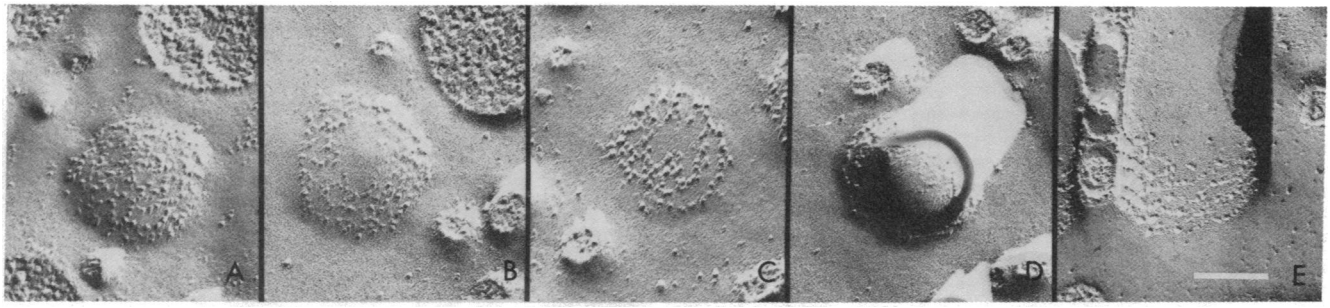

FIG. 2. Freeze-fracture preparations showing the developmental sequence of differentiation of the ciliary necklace during ciliogenesis in normal human nasal epithelium. (*A*) Aggregation of membrane-associated particles into patches approximately the diameter of a cilium. Note the random organization of particles in the patch. (*B* and *C*) Organization of randomly distributed particles into concentric arrays. (*D*) Emergence of new cilium revealed as a bud-like structure with necklace particles at its base. (*E*) Mature cilium with basal ciliary necklace. (Bar = 0.1 μm.)

estimate of the new ciliary population resulting from the emergence of new cilia, as indicated by the occurrence of both PNPs and existing cilia.

Statistical analyses of these categories indicated a significant difference in both ciliary density and spacing parameters between type A-*control* and type B-*real* categories ($P < 0.05$), reflecting the absence of an optimal distribution of cilia on type B faces. Similar tests comparing these parameters between type B-*real* and type B-*predicted* categories also indicated a statistically significant difference, suggesting the development of new ciliary spatial characteristics on the type B lumenal border. Given that some type A profiles contained a minimal number of PNPs, a statistical comparison of the ciliary distribution parameters of type A-*control* profiles with type B-*predicted* profiles would be inappropriate because type B profiles, with their varying distributions of PNPs, presumably evolve into mature optimal density ciliary beds, thus making them indistinguishable from type A profiles. However, it can be seen from the data presented in Table 1 that values for both ciliary density and interaxonemal spacing of the type B-*predicted* category are shifted toward those values indicated for type A-*control* profiles.

The variability of ciliogenic activity as observed in freeze-fracture preparations ranged from marked ciliogenesis on some lumenal borders to considerably lower levels in other cells, suggestive of the establishment of a specific density or spacing (or both) of cilia in differentiating cells. The critical nature of ciliary density and spacing factors was further suggested by observations of singular PNPs that occurred in small cilia-free spaces of lumenal membrane already having near optimal distributions of previously emerged cilia.

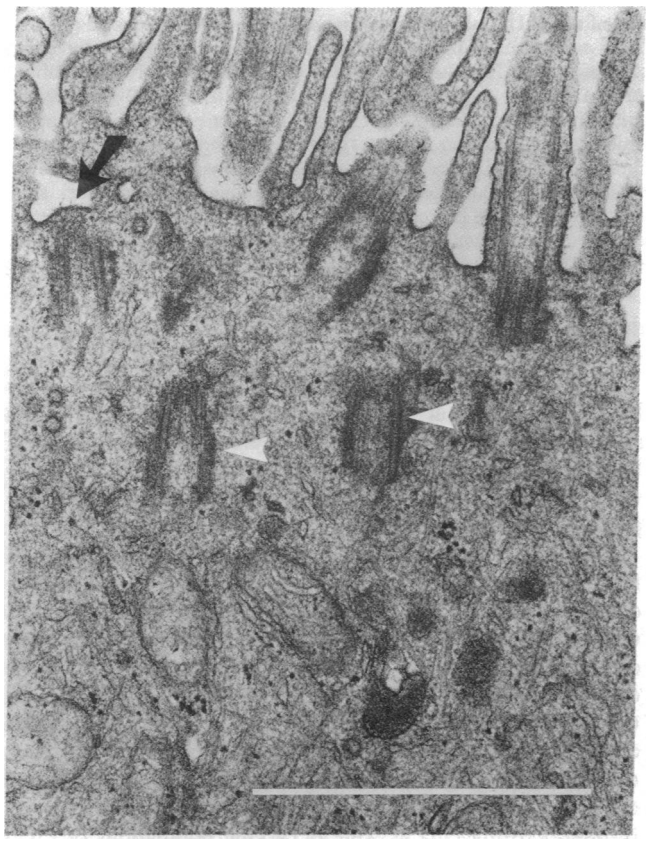

FIG. 3. Ultrathin section illustrating a bud (black arrow) of an emergent cilium at a basal body along the lumenal border of an epithelial cell heavily populated by microvilli. Also note two sublumenal basal bodies (white arrows). (Bar = 1.0 μm.)

DISCUSSION

Particle arrays similar to those described here have been observed by others in thymic cysts of experimental animals and were considered as evidence of active ciliogenesis (7). However, the ultrastructural characterization of nonembryological ciliogenesis in normal human epithelium and the evaluation of ciliary distribution have not been addressed previously in studies of this type. The development of these particle complexes during differentiation of cells in normal human nasal epithelium is particularly noteworthy due to the apparent density-dependent nature of their distribution. These observations suggest that the density of cilia on the lumenal border is a functionally significant characteristic relating to mucociliary clearance. The mechanics by which ciliary density is established or regulated, or both, are as yet poorly understood.

The characterization of these particle complexes as the progenitors of ciliary necklace particles and as indicators of imminent ciliogenesis is based on several criteria. First, the di-

Table 1. Morphometric analyses of ciliary distribution on human nasal epithelium

Profile type	Lumenal area analyzed, μm^2	Morphometric category	Ciliary density, $\frac{\text{cilia}}{\mu m^2}$ ± SD/μm^2	Interaxonemal spacing, $\overline{\mu m}$ ± SD
A	226.77	*Control*	3.72 ± 1.00	0.41 ± 0.05
B	203.19	*Real*	1.60 ± 0.33	0.49 ± 0.04
		Predicted	2.37 ± 0.39	0.43 ± 0.02

Control, existing cilia only; *real*, existing cilia only; *predicted*, existing cilia plus PNPs.

ameter of each complex is compatible with the diameter of a cilium. Also, these complexes have not been observed to be associated with any lateral or sublumenal membranes or with the lumenal membranes of any nonciliated cell type (i.e., goblet or brush border cells). The complexes appear frequently highly organized in the concentric alignment of their particles, an orientation inconsistent with degrading ciliary necklace structure that has been reported (8). Finally, the observations made on freeze-fracture preparations correlated well with parallel observations of ultrathin sections of human nasal epithelium in the appearance of ciliary buds and cytoplasmically distributed basal bodies in lumenal border cells, suggestive of active ciliogenesis.

It has been recognized that subcellular alterations and damage to epithelial cell cilia in airways can occur in response to infectious agents (8, 9) and air pollutant exposure (10, 11). Because the nasal vestibular region is the first site of interaction of toxic and infectious agents with the respiratory system, the epithelium lining this area may often be subjected to injurious challenges, thus requiring more active regenerative processes. It is also noteworthy that, like the lower gastrointestinal tract, the nasal mucosa is normally colonized by a microbial flora and may be subject to a similarly rapid epithelial cell turnover (12, 13) in contrast to the relatively slower turnover occurring in the normally sterile lower respiratory tract (14). Furthermore, parallel observations of human and experimental animal tracheal epithelium revealed that PNP arrays do occur in normal airway epithelium lining the lower respiratory tract, however, they are generally less abundant than in nasal epithelium. Such observations by others and the investigations carried out in this laboratory have raised the interesting question of the likelihood of continual ciliary generation in differentiated lumenal border cells. The frequency and abundance with which PNPs appear in nasal epithelium suggest this possibility as well as that of rapid differentiation of new cells. However, studies on human subjects do not permit the controls to more adequately approach this problem. This is an important and fundamental question of epithelial cell dynamics that is likely amenable to and should be addressed by appropriate experimental models in future studies.

In summary, these studies have demonstrated a well-organized sequence of differentiation of new ciliary membranes occurring during ciliogenesis in normal adult human nasal epithelium. The emergence of new cilia is preceded by the appearance and differentiation of intramembrane particle complexes with specific spatial characteristics. The development of optimal density ciliary populations on lumenal borders of the respiratory airways may have important consequences in the effective functioning of the mucociliary escalator.

The authors thank Dr. Wallace A. Clyde, Jr., for his review and comments in the preparation of this manuscript, Ms. Diane Fairclough for assistance with statistical analyses, Ms. S. S. Hu for technical assistance, and Mrs. Leigh Morrison for secretarial assistance. This research was supported by National Heart, Lung, and Blood Institute, Specialized Center of Research Grant HL19171-04 and Environmental Protection Agency Contract 68-02-3404. M.R.K. is a Parker B. Francis Fellow.

1. Sorokin, S. P. (1968) *J. Cell Sci.* **3**, 207–230.
2. Kanda, T. & Hilding, D. (1968) *Acta Oto-Laryngol.* **65**, 611–624.
3. Kalnins, V. I., Chung, C. K. & Turnbull, C. (1972) *Z. Zellforsch.* **135**, 461–471.
4. Breeze, R. G. & Wheeldon, E. B. (1977) *Am. Rev. Respir. Dis.* **116**, 705–777.
5. Gilula, N. B. & Satir, P. (1972) *J. Cell Biol.* **53**, 494–509.
6. Alford, B. R., Douglas, R. G., Jr. & Couch, R. B. (1969) *Arch. Otolaryngol.* **90**, 88–92.
7. Cordier, A. C. & Haumont, S. (1979) *Am. J. Anat.* **156**, 91–97.
8. Carson, J. L., Collier, A. M. & Clyde, W. A., Jr. (1979) *Science* **206**, 349–351.
9. Muse, K. E., Collier, A. M. & Baseman, J. B. (1977) *J. Infect. Dis.* **136**, 768–777.
10. Castleman, W. L., Tyler, W. S. & Dungworth, D. L. (1977) *Exp. Mol. Pathol.* **26**, 384–400.
11. Mellick, P. W., Dungworth, D. L., Schwartz, L. W. & Tyler, W. S. (1977) *Lab. Invest.* **36**, 82–90.
12. Cheng, H. & Leblond, C. P. (1974) *Am. J. Anat.* **141**, 461–480.
13. Abrams, G. D., Bauer, H. & Sprinz, H. (1963) *Lab. Invest.* **12**, 355–364.
14. Fabrikant, J. I. (1970) *Br. J. Cancer* **24**, 122–127.